Estuarine, Coastal and Shelf Science 96 (2012) 219–227

Contents lists available at SciVerse ScienceDirect

Estuarine, Coastal and Shelf Science

journal homepage: www.elsevier.com/locate/ecss

Assessing impacts of sea level rise on river salinity in the Gorai river network, Bangladesh

Md. Jabed Abdul Naser Bhuiyan [a,*], Dushmanta Dutta [a,b]

[a] SASE, Monash University, Northways road, Churchill, VIC 3842, Australia
[b] CSIRO Land and Water, ACT, Australia

ARTICLE INFO

Article history:
Received 23 November 2010
Accepted 3 November 2011
Available online 12 November 2011

Keywords:
advection–dispersion
hydrodynamic model
salinity
sea level rise
water level

ABSTRACT

Coastal zones are particularly vulnerable to climate change effects. Over the last century, sea level rose on average by 10–12 cm per decade and did so at much higher rates in some coastal areas due to land subsidence. The 4th IPCC report highlights the increased vulnerability of the coastal zones around the world due to sea level rises in 21st Century. Key concerns due to sea level rise include flooding and salinisation and its implications for water resources. Rising sea level increases the salinity of both surface water and ground water through salt water intrusion.

It is important to determine the impacts of sea level rise on salinity to devise suitable adaptation and mitigation measures and reduce impacts of salinity intrusion in coastal cities. The paper presents the outcomes of a study conducted in the coastal area of Gorai river network in the South West region of Bangladesh for developing a comprehensive understanding of the possible effects of sea level rise with the aid of a hydrodynamic model. A newly developed salinity flux model has been integrated with an existing hydrodynamic model in order to simulate flood and salinity in the complex waterways in the coastal zone of Gorai river basin. The integrated model has been calibrated and validated by numerous comparisons with measurements (tide, salinity). The model has been applied for future scenarios with sea level rise and the results obtained indicate the risk and changes in salinity. Due to sea level rise, the salinity has increased in the river and salinity intrusion length has also increased. Sea level rise of 59 cm produced a change of 0.9 ppt at a distance of 80 km upstream of river mouth, corresponding to a climatic effect of 1.5 ppt per meter sea level rise.

1. Introduction

Coastal and shallow marine regions are among the most productive systems in the world (Mann, 1988; Glantz, 1992). The Intergovernmental Panel on Climate Change (IPCC) in its fourth assessment report presents some observational evidence of climate change in the coastal regions. Some of the evidence includes increased ocean temperature, changes in precipitation, corresponding upstream river discharge and rising sea level. This will generally lead to higher coastal flooding and increased salinity (Parry, 2007).

Flood magnitudes and frequencies will very likely increase in most regions – mainly as a result of increased precipitation intensity and variability – and increasing temperatures are expected to intensify the climate's hydrologic cycle and melt snowpacks more rapidly (Parry, 2007). Flooding can affect water quality, as large volumes of flood water can transport contaminants into water bodies.

The lives of human beings and aquatic plants and animals are highly dependent on the availability of fresh water and rise in sea level can affect the availability and distribution of fresh water. Maintaining water quality is an on-going problem in the coastal zones which is expected to be exacerbated by climate change and sea level rise (SLR). SLR may also affect freshwater quality by increasing the salinity of coastal rivers and bays and causing salt water intrusion. Salt water intrusion is an important phenomenon in coastal zones, and can constitute a serious problem to society due to the need for fresh water for households, industry, or agriculture (Zhang et al., 2011). Salt water may infiltrate into coastal aquifers and movement of saline water into fresh ground water resources in coastal regions can result in decreasing water quality (Bashar and Hossain, 2006). Higher salt levels in the coastal region would also contaminate urban surface water supplies. As sea level rises the tidal salt water zone will penetrate further upstream. This zone therefore becomes unfit for cultivation, over a longer period of the annual cycle (Gornitz, 1991). Hilton et al. (2008) and Najjar et al.

* Corresponding author.
E-mail address: Jabed.Bhuiyan@monash.edu (M.J.A.N. Bhuiyan).

0272-7714/$ – see front matter © 2011 Elsevier Ltd. All rights reserved.
doi:10.1016/j.ecss.2011.11.005

(2010) reported a study to quantify salinity variations due to SLR in Chesapeake Bay, United States. The results obtained from hydrodynamic (HD) model simulations show salinity sensitivity to SLR of about 2 m^{-1} in this region (a salinity increase of 0.4 indicates chloride increase of 210 mgl^{-1}). Assessing coastal vulnerability to SLR has also been addressed globally in several recent studies (Van der Meulen et al., 1991; Thumerer et al., 2000; Wu et al., 2002; Kumar, 2006; Kleinosky et al., 2007).

The Gorai river and its tributaries, which flow through South West region of Bangladesh is particularly vulnerable to flooding due to its low-lying lands and very poor flood protection systems. Flow in the Gorai river, a tributary of the river Ganges, reduces during the dry season. Due to the reduced flow of the rivers in this area in dry season, salinity intrudes into the river systems. There is clear evidence of increased saline intrusion in the coastal zones of Bangladesh. For example, in the coastal city of Khulna the main power station uses fresh water to cool its boilers by sending a barge upstream to get fresh water. Over the last decade the barge has had to go further and further upstream in search of suitable fresh water for the purpose (NAPA, 2005). Increased salinity intrusion due to SLR poses a great threat to the Sundarban forest which covers a large area in the downstream part near Bay of Bengal. The Sundarban has already been affected due to reduced freshwater flowing through the Ganges river system over the last few decades particularly during the dry season. This has led to a definite inward intrusion of the salinity front affecting various species of plants and animals to be adversely affected. Increased salt water intrusion is considered as one of the main causes of death of Sundari trees (Shamsuddoha and Chowdhury, 2007).

The consequences of increased salinity are many and varied. Reduction of soil fertility results in low crop yield, hampering tree production etc. Miah et al. (2004) show that native fresh water fish species are disappearing gradually. Increased salinity has already reduced the farmers' interest of land cultivation. Groundwater which is the main source of drinking water has also been affected by increased salinity.

Computer based mathematical models are well recognized tools for simulating these complex problems. Mathematical models have been utilized for more than three decades (Dutta, 1999). Haralambidou et al. (2010) in their paper emphasized the necessity of physically based model to forecast the response of the coastal system to the variable external forces. Traditional lumped conceptual type models cannot rightfully be claimed to be scientifically sound (Klemes, 1988). This study aims to develop a comprehensive understanding of the impact of SLR on coastal water salinity with the aid of the hydrodynamic and advection–dispersion models. The objective of this paper is to develop a salinity flux model and integrate this with an existing hydrodynamic model. The integrated model is then used to assess the impact of SLR on salinity in the coastal zone rivers. Note that most of the existing salinity models are coupled with a hydrologic model such as SWIM (Krysanova et al., 1998). In this study, a hydrodynamic model (HD) has been used instead of a hydrologic model to represent the flow dynamics on overland and river systems in coastal regions. The HD model uses the concept of fully dynamic flow behavior and is most suitable for complex river systems in coastal zones (Dutta et al., 2007). The newly developed salinity model can take into account of salinity effect from both upstream and downstream. The overall framework of this study has been depicted here below (Fig. 1).

2. Sea level rise projection

Increasing concentration of greenhouse gases in the atmosphere is raising the atmospheric temperature. One of the direct and major consequences of increasing temperature is a rise in sea level. In the South Asian region, the current rise in sea level is reported to be about 0.001 meter per year (in India and Pakistan) (Ali, 1996). Global average SLR for 1990–2100 is projected to be 0.09–0.88 m according to the IPCC Third Assessment Report (TAR). Warrick et al. (1996) in the Second Assessment Report (SAR) predicted a similar range of 0.20–0.86 m by the year 2100 from the 1990 sea level. According to Solomon (2007) Fourth Assessment Report (FAR), global SLR is projected in the range of 0.18–0.59 m between 1980 to 1999 and 2090 to 2099. Due to the uncertainty of ice sheet discharge and based on recent evidence of acceleration in Greenland and Antarctica, FAR assumes a rise of about 1 m by the year 2100. One pilot study report prepared by the Department of Environment, Government of Bangladesh shows two estimates of potential future SLR of 0.30–1.5 m and 0.3–0.5 m in 2050 for Bangladesh (DOE, 1993).

3. Hydrodynamic model

The HD model was originally developed at the Public Work Research Institute (PWRI) of Japan (Yoshimoto et al., 1992). The model has two major components: a one dimensional river flow component and a two dimensional floodplain component. The main characteristic of the model is the coupling between the river and floodplain components and dynamic flow exchange through the links. The flow exchange between the river and floodplain may occur for various scenarios such as levee failure or overtopping, flow through structures such as pump or sluice gate, etc. Points and extent of flood levee failure is governed by the water level in the river and the height of levee through the use of unsteady flow calculation in the river. The model uses the one dimensional unsteady dynamic wave form of St Venant's equation for river flow simulation and two dimensional unsteady equations for floodplain flow. These governing equations, derived from the continuity and momentum equations, are solved using explicit solution schemes. The river nodes and floodplain grids are linked through suitable conceptual equations representing different conditions of flow exchange. The continuity and momentum equations used for flow routing in the river channel are described below as shown in Dutta et al. (2007).

$$\frac{dA}{dt} + \frac{dQ}{dx} = q \tag{1}$$

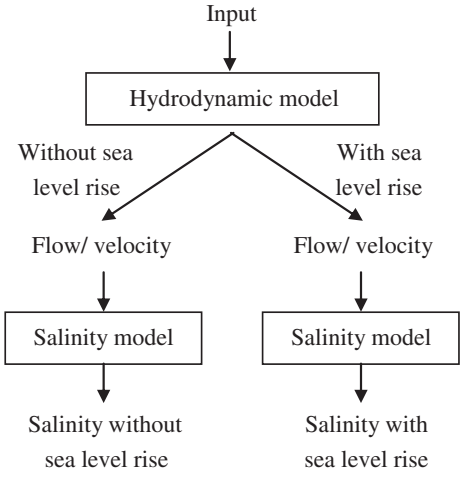

Fig. 1. Research framework of the study.

$$A\frac{dQ}{dt}+Q^2\frac{d\beta}{dx}-2\beta Q\frac{dA}{dt}-\frac{\beta Q^2}{A}\frac{dA}{dx}+gA^2\frac{dH}{dx}+gA^2\frac{Q^2}{\left[\sum\frac{A}{n}R^{2/3}\right]^2}=0 \tag{2}$$

Where, A = river cross-sectional area; Q = discharge through A; H = water level; R = hydraulic radius; t = time; x = distance along the longitudinal axis of the water course; q = lateral inflow or outflow; β = momentum factor; g = gravitational acceleration constant and n = Manning's roughness coefficient.

In the explicit solution scheme, a system of staggered grids is used, where water level and discharge are calculated in every alternate grid by solving the continuity and momentum equations. The water level at water level node (except downstream boundary node) is calculated numerically using finite difference forms of the continuity equation as presented below.

$$h_i^{t+1}=h_i^t+\frac{Q^t\Delta t}{A_s} \tag{3}$$

$$Q^t=\left\{\left(Q_{i-1}^t+q_{i-1}^t\right)+\left(Q_{c_{i-1}}^t+q_{c_{i-1}}^t\right)\right\}+\left\{\left(Q_{c_i}^t+q_{c_i}^t\right)+q_i^t\right\}-Q_{i+1}^t-Q_{s_i}^t \tag{4}$$

$$A_s=b_1X_{i-1}+b_2X_i+cfa+spa \tag{5}$$

Where, Q = sum of discharge at node i; A_s = surface area at node i; Q_i = discharge at node i; Q_{c_i} = discharge from confluence contribution to node i; Q_{s_i} = discharge for diversion at node i; q_i = lateral flow at node i; q_{c_i} = lateral flow to confluence contribution to node i; h_i = water level at node i; t = time suffix at known level; $t+1$ = time suffix at unknown level (calculation time); X_{i-1} = distance between $i-1$ (upstream node) and i nodes; b_1 = average width between $i-1$ and i nodes; b_2 = average width between i and $i-1$ nodes; cfa = surface area for confluence; spa = surface area for diversion.

The water level at discharge node (except upstream boundary) is calculated from the adjacent water level node by linear extrapolation. The discharge at discharge node is calculated using the momentum equation. The finite difference form of the momentum equation as described in Dutta et al. (2007) is follows;

$$Q_i^{t+1}=\frac{\left\|\frac{A_i^{t+1}Q_i^t}{\Delta t}-Q_i^{t2}\frac{\beta_i^{t+1}-\beta_{i-2}^{t+1}}{x_{i-1}+x_{i-2}}+2\beta_i^tQ_i^t\frac{A_i^{t+1}-A_i^t}{\Delta t}+\frac{\beta_i^{t+1}Q_i^{t2}}{A_i^t}\frac{A_i^{t+1}-A_{i-2}^{t+1}}{x_{i-1}+x_{i-2}}-gA_i^{(t+1)^2}\frac{H_{i+1}^{t+1}-H_{i-1}^{t+1}}{x_i+x_{i-1}}\right\|}{\left[\frac{A_i^{t+1}}{\Delta t}+\frac{gA_i^{(t+1)^2}|Q_i^t|}{\left(\sum_k\frac{A_{ik}}{n_k}R_{ik}^{2/3}\right)^2}\right]} \tag{6}$$

Where, A_i^t = cross sectional area for node i at time t; β_i^t = momentum factor for node i at time t; H_i^t = water level for node i at time t; Q_i^t = discharge for node i at time t; R_{ik} = hydraulic radius at node i; k = 2, (1 = minor bed x-section and 2 = major bed x-section); n_k = Manning's roughness coefficient for k; Δt = time step; g = gravitational acceleration constant; x_{i-2} = length of the channel segment between nodes $i-2$ and $i-1$; x_{i-1} = length of the channel segment between nodes $i-1$ and i; x_i = length of the channel segment between nodes i and $i+1$; $(i-2)$, $(i-1)$, i, $(i-1)$, …, $(i-n)$ = corresponding nodes in a segment from upstream to downstream.

The discharge at water level node is approximated by taking the average value of the discharge of the immediate upstream and downstream discharge nodes. The discharge for the last node of a main or diversion channel is assigned as the same discharge of the previous discharge node.

4. River salinity transport model

A salinity transport model has been developed to investigate transport processes in the river system of a coastal zone through estimating the advection–dispersion coefficients and integrated with the existing HD model. Both of the models work in FORTRAN environment.

As the depths of river in Gorai and other tributaries are small relative to width, vertical stratification can be neglected. When fresh water discharge increases, the strong downriver flow not only depresses salinity throughout the estuary, but also reduces the stratification as a result of increased vertical mixing and weakened two-layered circulation (Liu et al., 2001; Kim et al., 2010). Zhang et al. (2011) explained the widely use of models which calculate only the cross-sectional average situation, such as Savenije (1986, 1989, 1993, and 2005), Aertsl et al. (2000), Brockway et al. (2006), Nguyen and Savenije (2006), Nguyen et al. (2008), etc. These models have the advantage of being simple. Moreover, the observed salinity data in the study area showed no information on vertical depth. As the density is not considered in the momentum equation, the salinity can be considered as a passive tracer. So the salinity cannot alter the flow by changing its density.

4.1. Governing equations

The transportation and dispersion of solute in the longitudinal case involve a mathematical representation in the form of the following single dimensional, partial differential equation (Fischer et al., 1979; Orlob, 1983; Henderson-Sellars et al., 1990; Young and Wallis, 1992), generally known by Fickian diffusion equation or advection–dispersion equation (ADE),

$$\frac{\partial C}{\partial t}+v\frac{\partial C}{\partial x}=D\frac{\partial^2C}{\partial x^2} \tag{7}$$

where, C = concentration of the solute; v = cross-sectional average longitudinal velocity (=Q/A); Q = discharge through river section; A = cross section area of the river section; and D = longitudinal dispersion coefficient.

The dispersion coefficient can be specified as a function of the flow velocity calculated by the following equation,

$$D=av^b \tag{8}$$

where, a = dispersion factor; b = a dimensionless exponent. This concept is used in MIKE 11 model when running advection–dispersion simulation (DHI, 2003).

4.2. Calculation methods

The finite difference method is a well-established numerical method, which has been applied for salinity transport modelling. Eq. (7) can be approximated by a system of partial differential equations. If the concentration at the previous time step (C^t) is used in approximating the advection and dispersion terms of the transport equation, the temporal discretization is said to be explicit, leading to the following form of the finite difference equation (Zheng and Bennett, 1995):

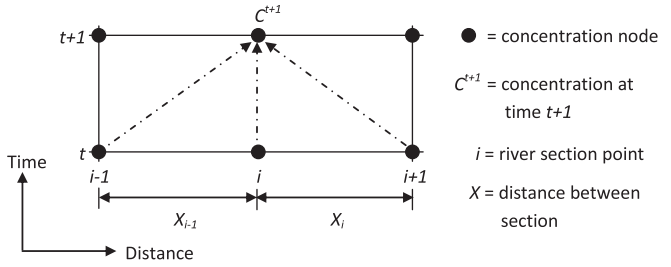

Fig. 2. Distance-time plane used in the solution scheme of salinity model (forward in time, central in space numerical).

$$C_i^{t+1} = C_i^t + \frac{D\Delta t}{(\Delta x)^2}\left(C_{i+1}^t - 2C_i^t + C_{i-1}^t\right) - \frac{v\Delta t}{\Delta x}\left[(1-\alpha)C_i^t + \alpha C_{i+1}^t - (1-\alpha)C_{i-1}^t - \alpha C_i^t\right] \quad (9)$$

where, C = salinity concentration; i = river section; t = time; D = dispersion coefficient; v = velocity, Δx = distance between section, α = spatial weighting factor.

In the explicit solution scheme a system of staggered grids is used, where salinity is calculated in every grid by solving the advection–dispersion equation. The distance-time ($x - t$) planes for formulating explicit finite difference schemes of advection–dispersion equation is shown in Fig. 2. At the junction, where tributary meets, the salinity and velocity at the upstream section is considered as the weighted average of the two upstream sections from two different rivers.

Here, water is considered to be completely mixed over the cross-sections and the dispersive transport is proportional to the concentration gradient. The approximation of advection - dispersion equation is dependent on the formulation of the St Venant's equation in the river. The technique uses the flow velocity (v) of the river which is calculated in the HD model.

5. Study area

The study area is the Gorai river basin located on the South West region of Bangladesh. It comprises an area between latitude 21°30' N to 24°00' N and longitude 88°50' E to 90°10' E. The area is bounded by Ganges river in the North, tributaries from Meghna River in the East, international boundary in the West and the Bay of Bengal in the South (Fig. 3). The annual average rainfall is 1,700 mm/year (ADB, 2005). The surface water system of the region consists of a numerous inter linked rivers, estuaries, and ephemeral water courses. The system mainly flows from North towards South and discharges to the Bay of Bengal. The availability of the surface water in the dry season is strongly dependent upon the inflow through the Gorai river. The topography of the region is rather flat, and gently sloping towards the Bay of Bengal. Sea salinity intrusion is a major concern in the southern part of the river system, as the

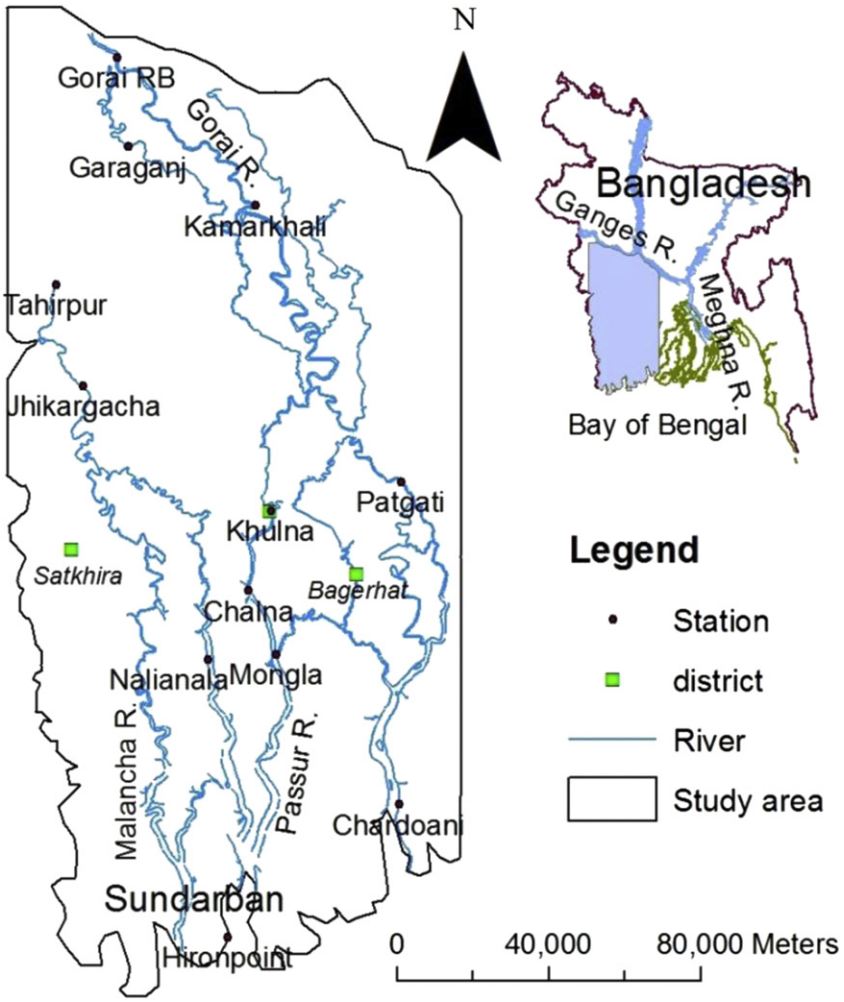

Fig. 3. South West region of Bangladesh.

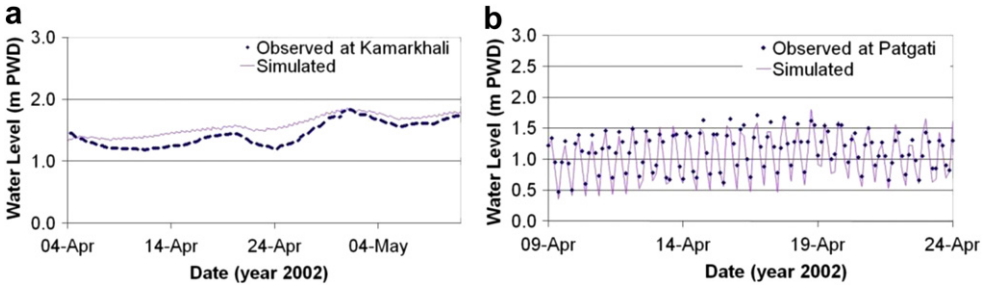

Fig. 4. Water level comparisons at (a) Kamarkhali and (b) Patgati in calibration.

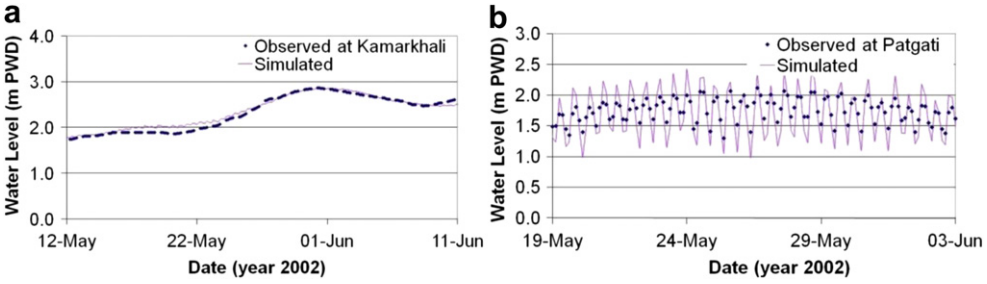

Fig. 5. Water level comparisons at (a) Kamarkhali and (b) Patgati in verification.

rivers are affected by tides and is an important issue in these rivers. Most of the area is protected with polders against river flooding. The downstream part of the area is covered with Sundarban forest.

6. Model setup, calibration and verification

The integrated model is simulated for several selected time periods in 2002 in the Gorai river basin. The topographical and other spatial data of the study area has been converted to a uniform grid network of 500 m mesh size for overland flow modeling. The existing polder heights have been added with the topography to represent the river bank protection. The total number of surface grids included in the HD model is 129,120. The Gorai river and its main tributaries have been included in the river network set up as shown in Fig. 3. Daily discharges at Gorai Railway Bridge, Garaganj and Jhikargacha stations are used as upstream boundary and three hourly water level data at Chardoani, Hironpoint and downstream point of Malancha river are used as downstream boundary. Daily rainfalls at 24 gauging stations are used as internal runoff. No lateral overland flow is considered. The river network data includes cross-section data at every 500 m to 5 km interval between Gorai Railway Bridge and the Bay of Bengal. The roughness coefficients for rivers and surface are estimated on the basis of the land use types (Dutta and Nakayama, 2009).

For the salinity model, observed salinity at Hironpoint (Fig. 3), Katka (downstream of Malancha river) and Dobaki South (near Chardoani) have been used as the downstream boundary conditions. No upstream boundary conditions are used in the salinity modeling due to non availability of observed data and it was kept as variable to assess the effects of changes in downstream salinity condition . All the necessary data for HD and salinity model have been collected from Bangladesh Water Development Board (BWDB) and the Institute of Water Modelling (IWM).

The HD model has been calibrated and verified for different events of the year 2002. The calibrated parameter is Manning's roughness in the river. The calibration and verification are

Table 1
Statistical indicators of HD model performance in calibration.

Station name	Observed WL (m PWD)		Computed WL (m PWD)		RRMSE	ABSERR (meter)	EF	R^2	PBIAS
	Max	Min	Max	Min					
Kamarkhali	1.83	1.18	1.84	1.34	0.143	0.152	0.319	0.425	−11.047
Patgati	1.8	0.38	1.88	0.36	0.179	0.164	0.617	0.792	8.116

Table 2
Statistical indicators of HD model performance in verification.

Station Name (period of simulation)	Observed WL (m PWD)		Computed WL (m PWD)		RRMSE	ABSERR (meter)	EF	R^2	PBIAS
	Max	Min	Max	Min					
Kamarkhali (May–June)	2.87	1.72	2.86	1.77	0.048	0.058	0.968	0.956	1.426
Patgati (May–June)	2.12	1.08	2.42	0.66	0.192	0.222	−0.128	0.527	2.98
Mongla (Nov–Dec)	2.56	−1.41	2.82	−0.70	0.793	0.483	0.656	0.692	−32.36

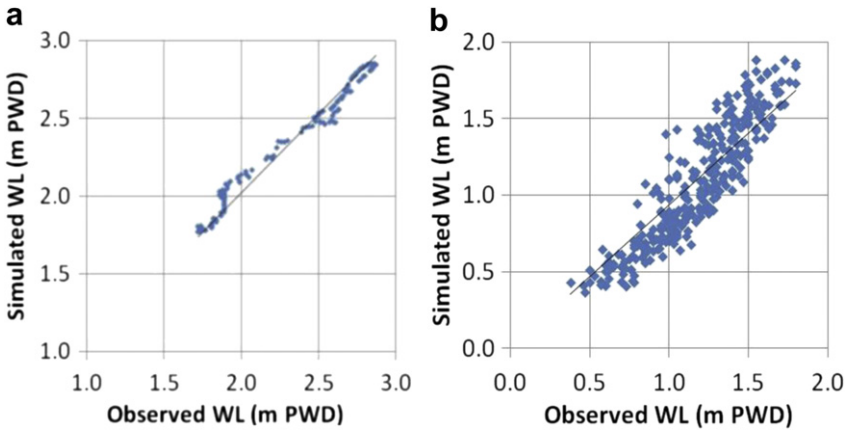

Fig. 6. Observed vs simulated water level at (a) Kamarkhali and (b) Patgati.

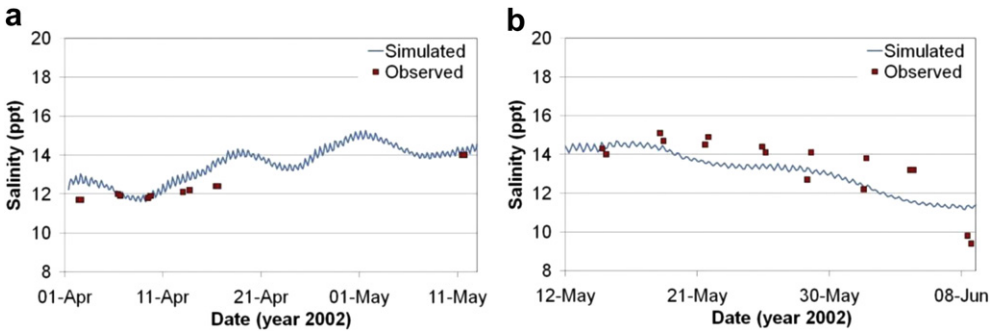

Fig. 7. Salinity comparison at Mongla in (a) calibration and (b) verification.

performed using the water level data at some selected stations. Dry period flow during the month of April and May in the year 2002 has been used for calibration. The roughness coefficients were adjusted by a trial and error approach. The coefficients were found to be within the range of 0.015–0.035 for all river sections. The coefficient is fixed for each section but varies for sections in other rivers. Fig. 4 shows the comparison of the simulated water level at different stations with the observed data where the water levels are measured based on the datum of the Public Works Department (PWD). The PWD datum is 0.46 m lower than the mean sea level (Tingsanchali and Karim, 2005).

For verification of the model parameter, water levels during the months of May–June and Nov–Dec 2002 have been considered. Fig. 5 shows the comparison of observed and simulated water levels at two stations, Kamarkhali and Patgati for the period of May–June. From the Figs. 4 and 5 it is seen that, the variability of water level in Patgati is obviously due to the tidal influence, while in the upstream Kamarkhali is mostly affected by river discharge.

The statistical indicators used for evaluating the performance of the model are: relative root mean squared error (RRMSE); mean absolute error (ABSERR); the Nash-Sutcliffe modeling efficiency index (EF); the goodness-of-fit (R^2) and the percentage (%) of deviation from observed streamflow (PBIAS). The equations used to determine these indicators are available in Stehr et al. (2008). Tables 1 and 2 give the values obtained for each of these indicators for the calibration and verification. The model performance has

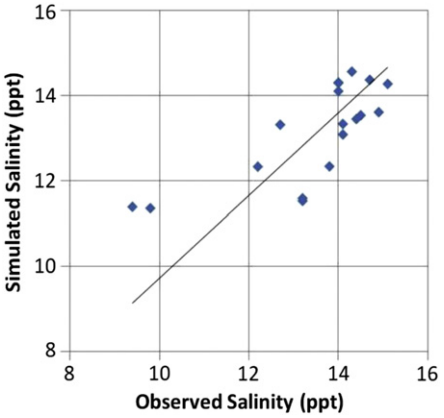

Fig. 8. Observed vs simulated Salinity at Mongla.

Table 3
Statistical indicators of Salinity model performance.

Model setup	Observed salinity (ppt)		Computed salinity (ppt)		RRMSE	ABSERR (meter)	EF	R^2	PBIAS
	Max	Min	Max	Min					
Calibration	12.4	11.7	13.8	11.8	0.233	0.640	−9.709	0.421	−5.134
Verification	15.1	9.4	14.6	11.3	0.291	0.897	0.526	0.567	2.295

Table 4
Model simulated maximum salinity.

Station	Without SLR (ppt)	With 59 cm SLR (ppt)	Salinity increase (ppt)
Mongla	14.8	15.7	0.9
Nalianala	17.3	18.0	0.7

been checked for water level at Kamarkhali, Patgati and Mongla during calibration and verification periods. The closer the values of RRMSE and ABSERR to zero, and those of R^2 and EF to unity, the better the model performance is evaluated (El-Nasr et al., 2005). For PBIAS, the optimal value is 0; a negative value indicates an overestimation of observed discharge values, whereas a positive value indicates underestimation.

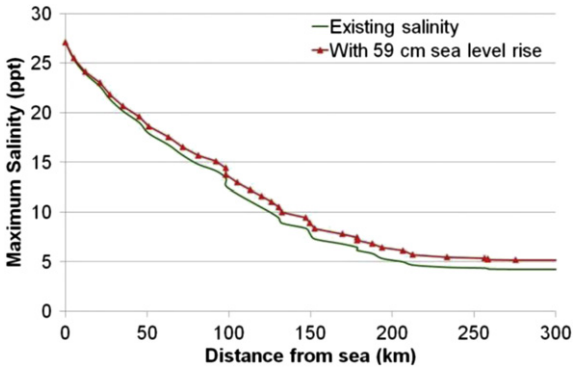

Fig. 9. Salinity long profile along Passur river.

From the water level comparison, it can be seen that during calibration of the HD model, the computed water level at Kamarkhali and Patgati are in good agreement (Fig. 4). For the verification period, the simulated water level at upstream station Kamarkhali shows good correlation with the observed water level (Fig. 5). The scatter plots of water levels of different stations together with the best fit lines are shown in Fig. 6. The results obtained demonstrate the high level of statistical correlation between observed and simulated water levels in both Kamarkhali and Patgati stations. The slope of water level correlations for Kamarkhali and Patgati are 1.01 and 0.94, respectively. These indicate that the model can estimate the water level at Kamarkhali fairly well; whereas the model slightly underestimates the water level at Patgati.

The salinity model has been calibrated by systematically adjusting the values of a selected system parameter to achieve an acceptable match between the measured salinity and the corresponding values predicted by the one dimensional advection–dispersion model. The calibration parameter is the dispersion coefficient in the river which is adjusted by trial and error. Fig. 7 shows the comparison of the observed and simulated salinity at the Mongla station during the calibration and verification period. Note that, the salinity data is presented in parts per thousand (ppt).

The statistical indicators for salinity model are summarized in Table 3. The model's performance has been checked for salinity at Mongla. The scatter plot of the observed vs. simulated salinity at Mongla is shown in Fig. 8. The dispersion coefficient varies with

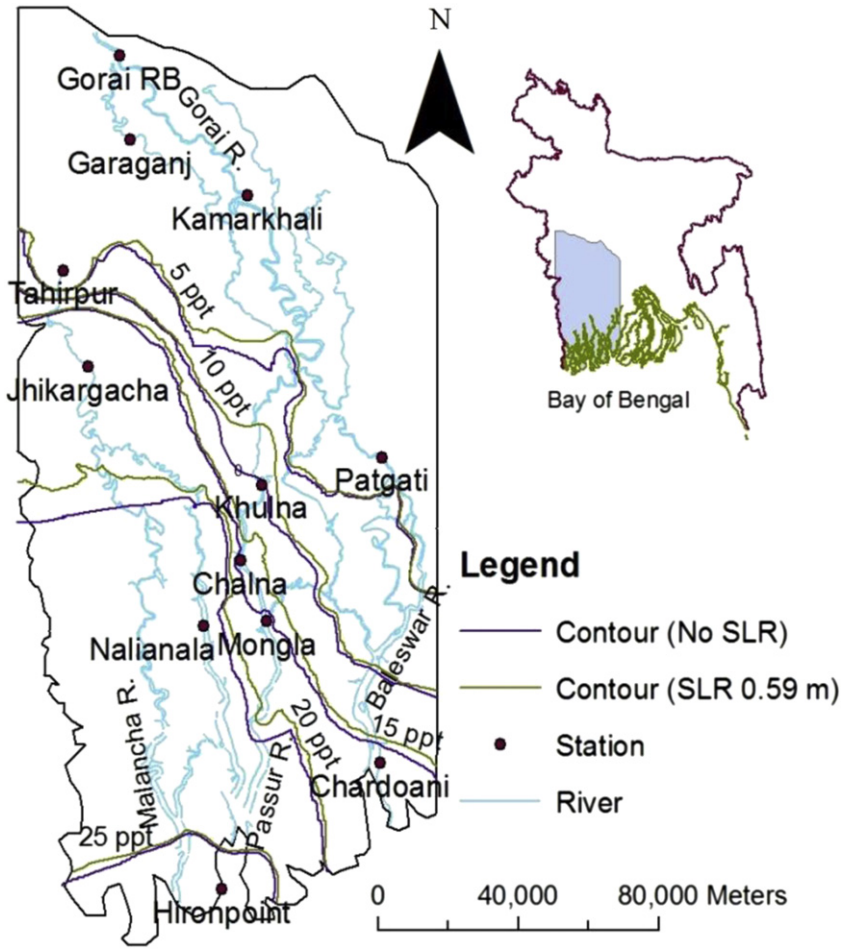

Fig. 10. Dry period maximum salinity contour line.

flow velocity but the coefficients (in Eq. 8) are kept constant for particular river section. The calibrated value of coefficient 'a' ranges from 2200 to 32000 for different sections and 'b' has been kept constant to 0.4 for all sections. The results show that the simulated salinity concentration follows a similar trend to the observed data. The slope of observed vs simulated salinity is 0.97 which shows that the model slightly underestimates the salinity at Mongla. The statistical correlation has demonstrated that the model is a reasonably efficient tool for describing and predicting sea water intrusion in coastal zone rivers.

7. Sea level rise impact

Considering the worst case scenario of IPCC fourth assessment report i.e. using SLR of 0.59 m, the integrated model has been applied in the same study area to simulate the worst possible impacts. In the calculations, the change in the downstream salinity (at Bay of Bengal) due to climate change has not been considered. Bhuiyan and Dutta (2009) show water level rise of 0.47 m and 0.58 m at Kamarkhali and Patgati respectively in dry season due to 0.59 m SLR. The changes in maximum salinity at different stations, due to the impact of the projected SLR have been given in Table 4. The results clearly show that the SLR impact on salinity intrusion is highly significant.

The longitudinal profile of the possible maximum salinity along the Passur river has been estimated. The profiles have been drawn in Fig. 9 first without considering SLR and subsequently taking the rise into account.

Based on maximum salinity for all the computing stations, salinity contour lines have been drawn. The summarized salinity contour lines for the entire study area have been shown in Fig. 10. These contour lines have been generated from simulated maximum salinities at different river sections. Note that, the computed salinity intrusion length of 10 ppt salinity line is 21 km upstream for the SLR.

8. Conclusion and discussion

A one dimensional advection–dispersion model has been developed and the performance of the model in Gorai river network has been presented in this paper. The SLR impact on salinity increase has been estimated with the integrated hydrodynamic and salinity model. The accuracy of the model results have been evaluated at the three stations for which time series of observed water level and salinity data were available. The evaluations are based on different statistical indicators and visual interpretation of observed *versus* modeled (calibration and verification) water level and salinity time series. The quality of the salinity model result depends on the quality of hydrodynamic simulation as the salinity model utilizes results obtained from the HD model. The water level comparisons in the upstream (Kamarkhali) and downstream locations (Patgati) show better relation. The Nash-Sutcliffe efficiency for Patgati water level and Mongla salinity show negative value because the residual variances are larger than the observed data variance. But it shows better performance for Mongla water level (Table 2). The statistical analysis of the salinity model shows that the model can be applied for long term analysis such as SLR. This indicates that the model is capable of measuring salinity in extreme cases (high salinity).

Reviewing the calibration results, both qualitatively (plotted time series inspection) and quantitatively (statistical analysis), it is clear that the selected approach performs well. The model is quite capable of reproducing the trends as well as the magnitude of salinity and its variations over a long period covering highly variable conditions in terms of both upstream river flow and downstream tidal amplitude. The adopted strategy and the qualities of the advection–dispersion results obtained dictate the model to be a powerful tool for modeling coastal zone rivers. The outcomes of the model show that the model can simulate the salinity and salt water intrusion along the river channels with a reasonable level of accuracy. The simulated water levels along the Gorai and Passur rivers show consistency with the observed data. The salinity transport mechanism is well considered in the model. On the whole, the computed results are reasonable.

There is, however, a limitation to the accuracy of this computation. Although the lateral inflow to the river from the floodplain is considered, the salinity from the floodplain is ignored. For further enhancement of the model, the lateral salt water inflow from the floodplain needs to be incorporated. The study implemented the impact in terms of salinity concentration and salt water intrusion. The model simulates salinity increment at Mongla to be 0.9 ppt due to 0.59 m SLR. This indicates salinity sensitivity to SLR of 0.9 ppt $\div$ 0.59 m = 1.5 ppt m^{-1}. Salinity front of 10 ppt line moves 21 km upstream in Passur river. The results also show that the salinity intrusion due to SLR is higher in the western part. This may happen due to lower discharges in those rivers as the river flow acts to push salt water towards the sea (Webster, 2010).

The increased salinity here could cause socio-economic problems. The saline water will be unsuitable for drinking and agricultural purposes. Salinity intrusion due to SLR will reduce agricultural output, especially rice because of the unavailability of fresh water and soil degradation. The rate of agricultural degradation is very high, with the impairment common for almost all rice fields in Khulna, Satkhira and Bagerhat districts.

Shrimp farming is one of the main businesses which will be negatively affected by increased salinity. SLR would change the location of the river estuary, causing a great change in fish habitat and breeding grounds. Penaid prawns breed and develop in brackish water, where fresh water and salt water mix. SLR would turn this interface backward, changing the habitat of prawns. Migration and unavailability of fresh water fishes may be detrimental to the fishing community of the region. SLR will play important role in erosion processes in the coastal zone which is one of the major causes of land loss. Land loss leads to loss of agricultural land, loss of road and other communication infrastructure and the loss of a wide range of biodiversity. Increased salinity may harm the growth of some species in Sundarban forest.

References

ADB, 2005. Southwest Area Integrated Water Resources Planning and Management Project in Bangladesh. Asian Development Bank, Bangladesh.

Aertsl, J.C.J.H., Hassan, A., Savenije, H.H.G., Khan, M.F., 2000. Using GIS tools and rapid assessment techniques for determining salt intrusion: STREAM a river basin management instrument. Physics and Chemistry of the Earth, Part B: Hydrology, Oceans and Atmosphere 25, 265–273.

Ali, A., 1996. Vulnerability of Bangladesh to climate change and sea level rise through tropical cyclones and storm surges. Water, Air, & Soil Pollution 92, 171–179.

Bashar, K.E., Hossain, M.A., 2006. Impact of sea level rise on salinity of coastal area of Bangladesh. 9th International River Symposium. Brisbane, Australia.

Bhuiyan, M.J.A.N. and Dutta, D., 2009. Sea level rise impacts on southwest coastal region Bangladesh using hydrodynamic model. Proceedings of the 32nd Hydrology and Water Resources Symposium. Engineers Australia, Newcastle, NSW, Australia, pp. 953–964.

Brockway, R., Bowers, D., Hoguane, A., Dove, V., Vassele, V., 2006. A note on salt intrusion in funnel-shaped estuaries: application to the Incomati estuary, Mozambique. Estuarine, Coastal and Shelf Science 66, 1–5.

DHI, 2003. MIKE 11 – A Modelling System for Rivers and Channels. Short Introduction Tutorial. DHI Water and Environment, pp. 5–27.

DOE, 1993. Assessment of the Vulnerability of Coastal Areas to Sea Level Rise and Other Effects of Global Climate Change. Pilot study Bangladesh, Report Prepared by Department of Environment. Govt. of Bangladesh, Dhaka.

Dutta, D., Nakayama, K., 2009. Effects of spatial grid resolution on river flow and surface inundation simulation by physically based distributed modelling approach. Hydrological Processes 23, 534–545.

Dutta, D., Alam, J., Umeda, K., Hayashi, M., Hironaka, S., 2007. A two-dimensional hydrodynamic model for flood inundation simulation: a case study in the lower Mekong river basin. Hydrological processes 21, 1223–1237.
Dutta, D., 1999. Distributed modeling of flood inundation and damage estimation. University of Tokyo, Japan, PhD thesis.
El-Nasr, A.A., Arnold, J.G., Feyen, J., Berlamont, J., 2005. Modelling the hydrology of a catchment using a distributed and a semi-distributed model. Hydrological Processes 19, 573–587.
Fischer, H.B., List, E.J., Koh, R.C.Y., Imberger, J., Brooks, N.H., 1979. Mixing in Inland and Coastal Waters. Academic Press Inc. (London) Ltd, New York, p. 302.
Glantz, M.H., 1992. Climate Variability, Climate Change, and Fisheries. Cambridge University Press, New York, p. 450.
Gornitz, V., 1991. Global coastal hazards from future sea level rise. Palaeogeography, Palaeoclimatology, Palaeoecology. (Global Planet. Change Sect.) 89, 379–398.
Haralambidou, K., Sylaios, G., Tsihrintzis, V.A., 2010. Salt-wedge propagation in a Mediterranean micro-tidal river mouth. Estuarine, Coastal and Shelf Science 90, 174–184.
Henderson-Sellars, B., Young, P.C., Ribeiro da Costa, J., 1990. Water Quality Models: Rivers and Reservoirs. In: Proceedings of 1988 International Symposium on Water Quality Modelling of Agricultural Non-Point Sources. United States Dept of Agriculture, Agricultural Research Service, United States, pp. 381–420.
Hilton, T.W., Najjar, R.G., Zhong, L., Li, M., 2008. Is there a signal of sea-level rise in Chesapeake Bay salinity? Journal of Geophysical Research 113, 1–12.
Kim, T., Sheng, Y.P., Park, K., 2010. Modeling water quality and hypoxia dynamics in Upper Charlotte Harbor, Florida, U.S.A. during 2000. Estuarine, Coastal and Shelf Science 90, 250–263.
Kleinosky, L.R., Yarnal, B., Fisher, A., 2007. Vulnerability of Hampton roads, Virginia to storm-surge flooding and sea level rise. Natural Hazards 40, 43–70.
Klemes, V., 1988. A hydrological perspective. Journal of Hydrology 100, 3–28.
Krysanova, V., Wohlfeil, D.I.M., Becker, A., 1998. Development and test of a spatially distributed hydrological/water quality model for mesoscale watersheds. Ecological Modelling 106, 261–289.
Kumar, P.K.D., 2006. Potential vulnerability implications of sea level rise for the coastal zones of Cochin, southwest coast of India. Environmental Monitoring and Assessment 123, 333–344.
Liu, W., Hsu, M., Kuo, A.Y., 2001. Investigation of long-term transport in Tanshui River estuary, Taiwan. Journal of Waterway, Port, Coastal and Ocean Engineering 127, 61–71.
Mann, K.H., 1988. Production and use of detritus in various freshwater, estuarine and coastal marine ecosystems. Limnology and Oceanography 33, 910–930.
Miah, M.Y., Mannan, M.A., Quddus, K.G., Mahmud, M.A.M., Baida, T., 2004. Salinity on cultivable land and its effects on crops. Pakistan Journal of Biological Sciences 7, 1322–1326.
Najjar, R.G., Pyke, C.R., Adams, M.B., Breitburg, D., Hershner, C., Kemp, M., Howarth, R., Mulholland, M.R., Paolisso, M., Secor, D., Sellner, K., Wardrop, D., Wood, R., 2010. Potential climate-change impacts on the Chesapeake Bay. Estuarine, Coastal and Shelf Science 86, 1–20.
NAPA, 2005. Formulation of Bangladesh Program of Action for Adaptation to Climate Change Project. Bangladesh Centre for Advance Studies (BCAS), Bangladesh.
Nguyen, A.D., Savenije, H.H.G., 2006. Salt intrusion in multi-channel estuaries: a case study in the Mekong Delta, Vietnam. Hydrology and Earth System Sciences 10, 743–754.
Nguyen, A.D., Savenije, H.H.G., Pham, D.N., Tang, D.T., 2008. Using salt intrusion measurements to determine the freshwater discharge distribution over the branches of a multi-channel estuary: the Mekong Delta case. Estuarine, Coastal and Shelf Science 77, 433–445.
Orlob, G.T. (Ed.), 1983. Mathematical Modelling of Water Quality: Streams, Lakes and Reservoirs. J. Wiley, Chichester.
Parry, M.L., 2007. Climate Change 2007: Impacts, Adaptation and Vulnerability: Contribution of Working Group II to the Fourth Assessment Report of the Intergovernmental Panel on Climate Change. Cambridge University Press, Cambridge, UK.
Savenije, H.H.G., 1986. A one-dimensional model for salinity intrusion in alluvial estuaries. Journal of Hydrology 85, 87–109.
Savenije, H.H.G., 1989. Salt intrusion model for high-water slack, low-water slack and mean tide on spread sheet. Journal of Hydrology 107, 9–18.
Savenije, H.H.G., 1993. Predictive model for salt intrusion in estuaries. Journal of Hydrology 148, 203–218.
Savenije, H.H.G., 2005. Salinity and Tides in Alluvial Estuaries. Elsevier, Amsterdam, p. 197.
Shamsuddoha, M., Chowdhury, R.K., 2007. Climate Change Impact and Disaster Vulnerabilities in the Coastal Areas of Bangladesh. Report prepared by Coast Trust and Equity and Justice Working Group (EJWG), Bangladesh.
Solomon, 2007. Climate Change 2007. The Physical Science Basis: Contribution of Working Group 1 to the Fourth Assessment Report of the Intergovernmental Panel on Climate Change. Cambridge University Press, Cambridge, United Kingdom and New York, NY, USA.
Stehr, A., Debels, P., Romero, F., Alcayaga, H., 2008. Hydrological modelling with SWAT under conditions of limited data availability: evaluation of results from a Chilean case study. (Modélisation hydrologique avec SWAT en conditions de données peu disponibles: évaluation des résultats d'une application au Chili). Hydrological Sciences Journal 53, 588–601.
Thumerer, T., Jones, A.P., Brown, D., 2000. A GIS based coastal management system for climate change associated flood risk assessment on the east coast of England. International Journal of Geographical Information Science 14, 265–281.
Tingsanchali, T., Karim, M.F., 2005. Flood hazard and risk analysis in the southwest region of Bangladesh. Hydrological Processes 19, 2055–2069.
Van der Meulen, F., Witter, J.V., Arens, S.M., 1991. The use of a GIS in assessing the impacts of sea level rise on nature conservation along the Dutch coast; 1990–2090. Landscape Ecology 6, 105–113.
Warrick, R.A., Le Provost, C., Meier, M.F., Oerlemans, J., Woodworth, P.L., 1996. Changes in Sea Level. In: Houghton, J.T., Meira Filho, L.G., Callander, B.A., Harris, N., Klattenberg, A., Maskell, K. (Eds.), Climate Change 1995, The Science Of Climate Change. Cambridg University Press, pp. 359–405.
Webster, I.T., 2010. The hydrodynamics and salinity regime of a coastal lagoon – The Coorong, Australia – Seasonal to multi-decadal timescales. Estuarine, Coastal and Shelf Science 90, 264–274.
Wu, S., Yarnal, B., Fisher, A., 2002. Vulnerability of coastal communities to sea-level rise: a case study of Cape May County, New Jersey, USA. Climate Research 22, 255–270.
Yoshimoto, T., Fueda, T., Ikeda, Y., Kawakami, T., 1992. Flood Simulation of Two Dimensional Unsteady Flood Model. Technical memorandum of Public Work Research Institute (PWRI), Public Works Research Institute, Japan. T. M. of PWRI No. 3105.
Young, P.C., Wallis, S.G., 1992. Solute transport and dispersion in channels, forthcoming. In: Beven, K.J., Kirby, M.J. (Eds.), Channel Networks. J. Wiley, Chichester.
Zhang, E., Savenije, H.H.G., Wu, H., Kong, Y., Zhu, J., 2011. Analytical solution for salt intrusion in the Yangtze Estuary, China. Estuarine, Coastal and Shelf Science 91, 492–501.
Zheng, C., Bennett, G.D., 1995. Applied Contaminant Transport Modeling, Theory and Practice. Van Nostrand Reinhold, a division of International Thomson Publishing Inc, New York, p. 440.